

APPENDIX A

Lateral-torsional buckling of composite beams for buildings

This appendix supplements the comments on *clause 6.4*.

Simplified expression for ‘cracked’ flexural stiffness of a composite slab

The ‘cracked’ stiffness per unit width of a composite slab is defined in *clause 6.4.2(6)* as the lower of the values at mid-span and at a support. The latter usually governs, because the profiled sheeting may be discontinuous at a support. It is now determined for the cross-section shown in Fig. A.1 with the sheeting neglected.

It is assumed that only the concrete within the troughs is in compression. Its transformed area in ‘steel’ units is

$$A_e = b_0 h_p / n b_s \tag{a}$$

where n is the modular ratio. The position of the elastic neutral axis is defined by the dimensions a and c , so that

$$A_e c = A_s a \quad \text{and} \quad a + c = z \tag{b}$$

where A_s is the area of top reinforcement per unit width of slab, and

$$z = h - d_s - h_p / 2 \tag{c}$$

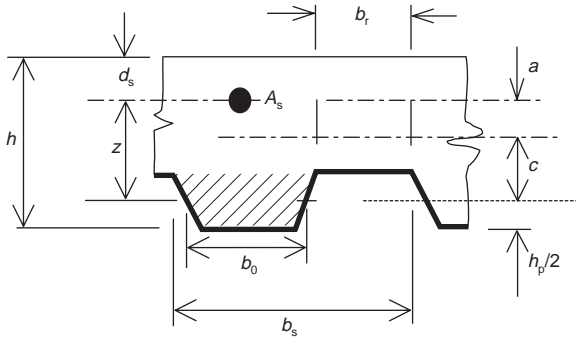


Fig. A.1. Model for stiffness of a composite slab in hogging bending



$$W_{pa} = \frac{(h-2t_f)t_w^2}{4} + \frac{2t_f b^2}{4} \quad (C.20)$$

and

$$W_{pc} = \frac{h_c b_c^2}{4} - W_{pa} - W_{ps} \quad (C.21)$$

For the different positions of the neutral axes, h_n and $W_{pa, n}$ are given by:

(a) Neutral axis in the web, $h_n \leq t_w/2$:

$$h_n = \frac{N_{pm, Rd} - A_{sn}(2f_{sd} - f_{cc})}{2h_c f_{cc} + 2h(2f_{yd} - f_{cc})} \quad (C.22)$$

$$W_{pa, n} = h h_n^2 \quad (C.23)$$

(b) Neutral axis in the flanges, $t_w/2 < h_n < b/2$:

$$h_n = \frac{N_{pm, Rd} - A_{sn}(2f_{sd} - f_{cc}) + t_w(2t_f - h)(2f_{yd} - f_{cc})}{2h_c f_{cc} + 4t_f(2f_{yd} - f_{cc})} \quad (C.24)$$

$$W_{pa, n} = 2t_f h_n^2 + \frac{(h-2t_f)t_w^2}{4} \quad (C.25)$$

(c) Neutral axis outside the steel section, $b/2 \leq h_n \leq b_c/2$

$$h_n = \frac{N_{pm, Rd} - A_{sn}(2f_{sd} - f_{cc}) - A_a(2f_{yd} - f_{cc})}{2h_c f_{cc}} \quad (C.26)$$

$$W_{pa, n} = W_{pa} \quad (C.27)$$

The plastic modulus of the concrete in the region of depth $2h_n$ then results from

$$W_{pc, n} = h_c h_n^2 - W_{pa, n} - W_{ps, n} \quad (C.28)$$

with $W_{ps, n}$ according to equation (C.19), changing the subscript z to y .

Concrete-filled circular and rectangular hollow sections

The following equations are derived for rectangular hollow sections with bending about the y -axis of the section (see Fig. C.3). For bending about the z -axis the dimensions h and b are to be exchanged as well as the subscripts z and y . Equations (C.29) to (C.33) may be used for circular hollow sections with good approximation by substituting

$$h = b = d \quad \text{and} \quad r = d/2 - t$$

$$W_{pc} = \frac{(b-2t)(h-2t)^2}{4} - \frac{2}{3}r^3 - r^2(4-\pi)(0.5h-t-r) - W_{ps} \quad (C.29)$$

with W_{ps} according to equation (C.9).

W_{pa} may be taken from tables, or be calculated from

$$W_{pa} = \frac{bh^2}{4} - \frac{2}{3}(r+t)^3 - (r+t)^2(4-\pi)(0.5h-t-r) - W_{pc} - W_{ps} \quad (C.30)$$

$$h_n = \frac{N_{pm, Rd} - A_{sn}(2f_{sd} - f_{cc})}{2bf_{cc} + 4t(2f_{yd} - f_{cc})} \quad (C.31)$$

$$W_{pc, n} = (b-2t)h_n^2 - W_{ps, n} \quad (C.32)$$

$$W_{pa, n} = bh_n^2 - W_{pc, n} - W_{ps, n} \quad (C.33)$$

with $W_{ps, n}$ according to equation (C.19).

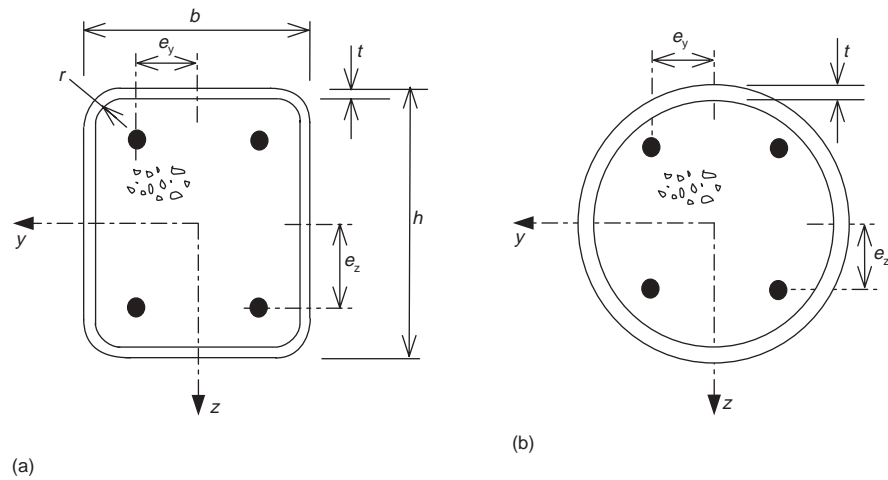


Fig. C.3. Concrete-filled (a) rectangular and (b) circular hollow sections, with notation

Example C.1: N - M interaction polygon for a column cross-section

The method of Appendix C is used to obtain the interaction polygon given in Fig. 6.38 for the concrete-encased H section shown in Fig. 6.37. The small area of longitudinal reinforcement is neglected. The data and symbols are as in Example 6.10 and Figs 6.37, C.1 and C.2.

Design strengths of the materials: $f_{yd} = 355 \text{ N/mm}^2$; $f_{cd} = 16.7 \text{ N/mm}^2$.

Other data: $A_a = 11\,400 \text{ mm}^2$; $A_c = 148\,600 \text{ mm}^2$; $t_f = 17.3 \text{ mm}$; $t_w = 10.5 \text{ mm}$; $b_c = h_c = 400 \text{ mm}$; $b = 256 \text{ mm}$; $h = 260 \text{ mm}$; $10^{-6} W_{pa,y} = 1.228 \text{ mm}^3$; $10^{-6} W_{pa,z} = 0.575 \text{ mm}^3$; $N_{pl,Rd} = \mathbf{6156 \text{ kN}}$.

Major-axis bending

From equation (C.8),

$$N_{pm,Rd} = 148.6 \times 16.7 = \mathbf{2482 \text{ kN}}$$

From equation (C.12),

$$h_n = 2482 / [0.8 \times 16.7 + 0.021 \times (710 - 16.7)] = 89 \text{ mm}$$

so the neutral axis is in the web (Fig. C.4(a)), as assumed. From equation (C.11), the plastic section modulus for the whole area of concrete is

$$10^{-6} W_{pc} = 4^3/4 - 1.228 = 14.77 \text{ mm}^3$$

From equation (C.13),

$$10^{-6} W_{pa,n} = 10.5 \times 0.089^2 = 0.083 \text{ mm}^3$$

From equation (C.18),

$$10^{-6} W_{pc,n} = 400 \times 0.089^2 - 0.083 = 3.085 \text{ mm}^3$$

From equation (C.5),

$$M_{max,Rd} = 1.228 \times 355 + 14.77 \times 16.7/2 = \mathbf{559 \text{ kN m}}$$

From equations (C.6) and (C.7),

$$M_{pl,Rd} = 559 - (0.083 \times 355 + 3.085 \times 16.7/2) = \mathbf{504 \text{ kN m}}$$

The results shown above in bold type are plotted on Fig. 6.38.

$$\tilde{\tilde{P}}_s(\xi_x, z = 0, \omega) = \frac{2\pi P_0}{c} \frac{\delta[\xi_z - (\omega - \omega_0)/c]}{(L_c \xi_x)^4 - (\omega/\Omega)^2 + 1} \tag{12.17}$$

The inverse Fourier transform into the space solution is

$$u_b(x, t) = \frac{1}{2\pi} \int_{-\infty}^{\infty} \frac{P_0}{c} \frac{\exp[-i(\omega - \omega_0)x/c] \exp(i\omega t)}{EI[(\omega - \omega_0)/c]^4 - \omega^2 m + \tilde{\tilde{K}}[(\omega - \omega_0)/c, \omega]} d\omega \tag{12.18}$$

in which a new parameter to define the ground stiffness,

$$\tilde{\tilde{K}}(\xi_x, \omega) = \frac{2B}{\tilde{\tilde{G}}_s(\xi_x, y = 0, z = 0, \omega)} \tag{12.19}$$

has been introduced for the inverse of the Green's function $\tilde{\tilde{G}}_s(\xi_x, y = 0, z = 0, \omega)$ for the soil.

Once the interaction force $P_s(\xi_x, y = 0, z = 0, \omega)$ is determined, then the ground motion at locations other than the interface at $y = 0, z = 0$ is obtained from

$$\tilde{\tilde{u}}_s(\xi_x, \xi_y, z, \omega) = \tilde{\tilde{G}}_z(\xi_x, \xi_y, z, \omega) \tilde{\tilde{P}}_s(\xi_x, z = 0, \omega) \tilde{\tilde{\Psi}}(\xi_y) \tag{12.20}$$

where

$$\tilde{\tilde{P}}_s(\xi_x, y = 0, z = 0, \omega) = \frac{2\pi P_0}{c} \tilde{\tilde{\Phi}}(\xi_x, \omega) \delta\left(\xi_x - \frac{\omega - \omega_0}{c}\right) \tag{12.21}$$

$$\tilde{\tilde{\Phi}}(\xi_x, \omega) = \frac{\tilde{\tilde{K}}(\xi_x, \omega)}{EI\xi_x^4 - m\omega^2 + \tilde{\tilde{K}}(\xi_x, \omega)} \tag{12.22}$$

where the ground Green's function $\tilde{\tilde{G}}_z(\xi_x, \xi_y, z, \omega)$ is defined for the x -, y - and z -directional response components. The wave field is calculated for the in-plane and out-of-plane motions and the respective contributions are converted to Cartesian coordinates using equation (12.67). Therefore, the final results are functions of the wavenumbers ξ_x and ξ_y .

If the soil impedance is assumed to be constant, i.e. $K(\xi_x, \omega) = K$, then

$$\tilde{\tilde{P}}_s(\xi_x, z = 0, \omega) = \frac{2\pi P_0}{c} \frac{\delta[\xi_x - (\omega - \omega_0)/c]}{(L_c \xi_x)^4 - (\omega/\Omega)^2 + 1} \tag{12.23}$$

where

$$L_c = \sqrt[4]{\frac{4EI}{K}} \tag{12.24}$$

$$\Omega = \sqrt{\frac{K}{m}} \tag{12.25}$$

For the frequency range $\omega/\Omega \ll 1$, the soil reaction is approximated by

$$\tilde{\tilde{P}}_s(\xi_x, y = 0, z = 0, \omega) = \frac{2\pi P_0}{c} \tilde{\tilde{\Phi}}(\xi_x) \delta\left(\xi_x - \frac{\omega - \omega_0}{c}\right) \tag{12.26}$$



in which y_0 gives the coordinate of the triangle apex, and B is its base width.

The Fourier transform of equation (12.29) can be expressed for a specific frequency ω_j , using equation (12.30), as

$$\tilde{\tilde{F}}_N(\xi_x, \xi_y, z, \omega) = \frac{2\pi}{c} \tilde{\Phi}(\xi_x) \tilde{\Psi}(\xi_y) \chi(\xi_x) \sum_j A_k(\omega_j) \delta\left(\xi_x - \frac{\omega - |\omega_j|}{c}\right) \delta(z) \quad (12.36)$$

where

$$\chi_N(\xi) = (1 + e^{ia\xi_x} + e^{i(a+b)\xi_x} + e^{i(2a+b)\xi_x}) \frac{1 - e^{iNL_7\xi_x}}{1 - e^{iL_7\xi_x}} \quad (12.37)$$

where $A_k(\omega_j)$ is the load intensity in the k direction at frequency ω_j . The Fourier transform of equation (12.35) is obtained as

$$\tilde{\Psi}(\xi_y) = \frac{4[1 - \cos(B\xi_y)]}{(B\xi_y)^2} \cos(\xi_y y_0) \quad (12.38)$$

The characteristic value is taken as $q = 1.5$ m in the later analysis in view of the conventional track structure. The coefficients $A_k(\omega_j)$ should be determined on the basis of matching the simulation results to measurement data (see, e.g., [12.20]). The response in the transformed domain can be solved for, as

$$\tilde{\tilde{u}}(\xi_x, \xi_y, z, \omega) = \mathbf{G}_z(\xi_x, \xi_y, z, \omega) \sum_j A(\omega_j) \delta\left(\xi_x - \frac{\omega - \omega_j}{c}\right) \quad (12.39)$$

where $\mathbf{G}_z(\xi_x, \xi_y, z, \omega)$ denotes the transformed-domain solution for the stationary load corresponding to equation (12.36). The computation of $\mathbf{G}_z(\xi_x, \xi_y, z, \omega)$ is formulated in the next section. The response in the space and time domain is therefore obtained from the inverse transform of

$$\begin{aligned} \mathbf{u}_s(x, y, z, t) = & \frac{1}{8\pi^3} \sum_j A(\omega_j) \int_{-\infty}^{\infty} \int_{-\infty}^{\infty} \tilde{\tilde{u}}\left(\frac{\omega - \omega_j}{c}, \xi_{yk}, z, \omega\right) \exp\left(i\frac{\omega_j x}{c}\right) \times \\ & \exp(-i\xi_y y) \exp\left[i\omega\left(t - \frac{x}{c}\right)\right] d\xi_y d\omega \end{aligned} \quad (12.40)$$

The discretized solution then follows according to equation (12.6). Hence,

$$\begin{aligned} \mathbf{u}_s(x, y, z, \omega) = & \frac{1}{4\pi^2} \sum_{k=0}^K \sum_j \tilde{\tilde{u}}_s\left(\frac{\omega - \omega_j}{c}, \xi_{yk}, z, \omega\right) A(\omega_j) \times \\ & \mathbf{G}_z\left(\frac{\omega - \omega_j}{c}, \xi_{yk}, z, \omega\right) \exp\left(-i\frac{\omega - \omega_j}{c} x\right) \Delta\xi_y \end{aligned} \quad (12.41)$$

where

$$\xi_{yk} = \frac{2\pi k}{L} \quad (k = 0, 1, 2, 3, \dots, K)$$

where $\Delta\xi_y = 2\pi/L$, L is a specific length.

12.2.5. Elastodynamic analysis

12.2.5.1. Three-dimensional wave motions [12.17, 12.19]

An inhomogeneous layered medium for which the properties are constant within individual layers of depths h is defined by the density ρ and the complex Lamé constants $\lambda^c = \lambda(1 + 2\zeta i)$ and $\mu^c = \mu(1 + 2\zeta i)$, where ζ is the internal damping ratio of the focused layer. The governing equation of an elastic body under the force action f is described by

$$\mu^c \tilde{u}_{i, jj} + (\lambda^c + \mu^c) \tilde{u}_{j, ji} + \omega^2 \rho \tilde{u}_i + \tilde{f}_i = 0 \quad (12.42)$$

where the subscripts i and j denote the space coordinates and the comma convention is used for space derivatives.

The resolution of the three-dimensional wave equation into the SV-P and the SH wave fields is performed via the relationship

$$\begin{Bmatrix} \tilde{u}_x \\ \tilde{u}_y \\ \tilde{u}_z \end{Bmatrix} = \begin{bmatrix} i\xi_x/\xi & 0 & -i\xi_y/\xi \\ i\xi_y/\xi & 0 & i\xi_x/\xi \\ 0 & 1 & 0 \end{bmatrix} \begin{Bmatrix} \tilde{u}_1 \\ \tilde{u}_2 \\ \tilde{u}_3 \end{Bmatrix} \quad \text{or} \quad \tilde{u}_{x,y,z} = \mathbf{C}\tilde{u}_{1,2,3} \quad (12.43)$$

where the subscripts 1 and 2 correspond to the coordinates in the transformed domain. Similar expressions hold for the force vectors as well:

$$\tilde{f}_{x,y,z} = \mathbf{C}\tilde{f}_{1,2,3} \quad (12.44)$$

Hence, the decoupled in-plane motions comprising the SV and P waves are governed by

$$\mu^c \frac{d^2 \tilde{u}_1}{dz^2} - (\lambda^c + 2\mu^c) k_\alpha^2 \tilde{u}_1 - (\lambda^c + \mu^c) \xi \frac{d\tilde{u}_2}{dz} = -\tilde{f}_1 \quad (12.45)$$

$$(\lambda^c + \mu^c) \xi \frac{d\tilde{u}_1}{dz} + (\lambda^c + 2\mu^c) \frac{d^2 \tilde{u}_2}{dz^2} - \mu^c k_\beta^2 \tilde{u}_2 = -\tilde{f}_2 \quad (12.46)$$

The out-of-plane motion comprising the SH wave is governed by

$$\mu^c \frac{d^2 \tilde{u}_3}{dz^2} - \mu^c k_\beta^2 \tilde{u}_3 = -\tilde{f}_3 \quad (12.47)$$

We define $V_p = \sqrt{[(\lambda^c + 2\mu^c)/\rho]}$ and $V_s = \sqrt{(\mu^c/\rho)}$ to denote the P-wave and the S-wave velocity, respectively. The notations

$$k_\alpha = \sqrt{\xi^2 - (\omega/V_p)^2}, \quad k_\beta = \sqrt{\xi^2 - (\omega/V_s)^2} \quad (12.48)$$

with $\xi^2 = \xi_x^2 + \xi_y^2$ have been introduced for defining the wavenumbers for the P-wave and the S-wave field, respectively.

The displacements obtained from the solution of equations (12.45) and (12.46) can be expressed as